RSC Advances

This is an *Accepted Manuscript*, which has been through the Royal Society of Chemistry peer review process and has been accepted for publication.

Accepted Manuscripts are published online shortly after acceptance, before technical editing, formatting and proof reading. Using this free service, authors can make their results available to the community, in citable form, before we publish the edited article. This *Accepted Manuscript* will be replaced by the edited, formatted and paginated article as soon as this is available.

You can find more information about *Accepted Manuscripts* in the Information for Authors.

Please note that technical editing may introduce minor changes to the text and/or graphics, which may alter content. The journal's standard Terms & Conditions and the Ethical guidelines still apply. In no event shall the Royal Society of Chemistry be held responsible for any errors or omissions in this *Accepted Manuscript* or any consequences arising from the use of any information it contains.

ROYAL SOCIETY OF CHEMISTRY

www.rsc.org/advances

Graphical abstract

Graphene oxide as a covalent-crosslink agent for EVM-g-PA6 thermoplastic elastomeric nanocomposites

Wenjing Wu[a,b], Chaoying Wan[c], Yong Zhang[a1]

[a] *State Key Laboratory of Metal Matrix Composites, School of Chemistry and Chemical Engineering, Shanghai Jiao Tong University, 200240,China*

[b] *Aerospace Research Institute of Materials & Processing Technology, 100076, Beijing, China*

[c] *International Institute for Nanocomposites Manufacturing, WMG, University of Warwick, CV4 7AL, UK*

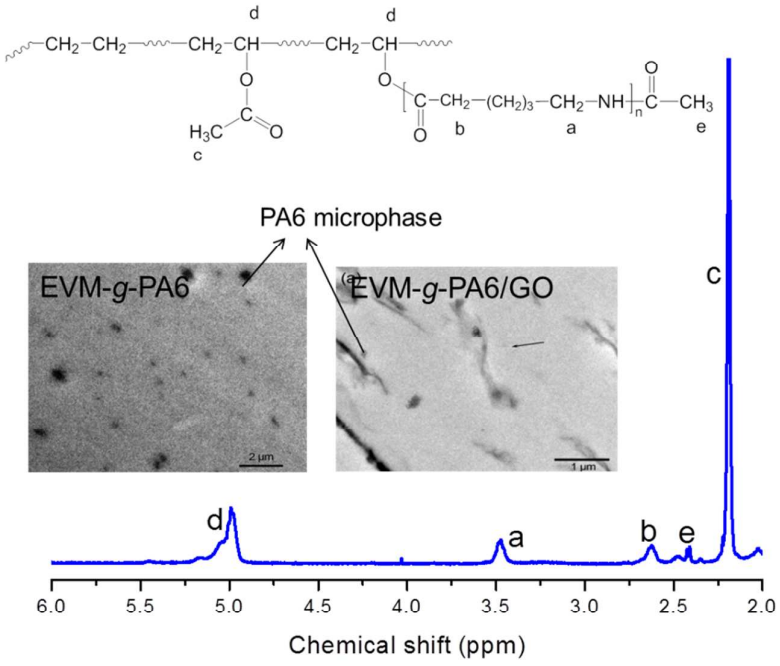

[1] *Corresponding author. Tel:* +86 21 54743257.
E-mail address: yong_zhang@sjtu.edu.cn (Y Zhang).

RSC Advances Accepted Manuscript

Graphene oxide as a covalent-crosslink agent for EVM-g-PA6 thermoplastic elastomeric nanocomposites

Wenjing Wu[a,b], Chaoying Wan[c], Yong Zhang[a1]

[a] *State Key Laboratory of Metal Matrix Composites, School of Chemistry and Chemical Engineering, Shanghai Jiao Tong University, 200240,China*

[b] *Aerospace Research Institute of Materials & Processing Technology, 100076, Beijing, China*

[c] *International Institute for Nanocomposites Manufacturing, WMG, University of Warwick, CV4 7AL, UK*

Abstract

A novel polyamide 6 grafted ethylene-vinyl acetate rubber copolymer (EVM-g-PA6) was synthesized in the presence of graphene oxide (GO). The reaction mechanisms of a sequential ring-opening ester-amide exchange reaction between caprolactam (CL) monomer and acetate groups of EVM with and without GO were proposed and investigated. Under the reaction conditions, the yield of the copolymer out of the CL/EVM (60/40) mixture was 26.4 wt% at 15% of the conversion of CL. The graft PA6 content was determined to be 4~6 wt%, and the grafting efficiency was further enhanced up to 13.1 wt% with the incorporation of 0.7 wt% of GO. This suggested that the GO accelerated the polymerization reaction of CL, and also acted as a crosslinking agent to bridge homopolymerised PA6 with EVM-g-PA6 copolymer. In addition, GO was thermally reduced *in situ* during the reaction process, thus significantly enhanced both the volume conductivity and permittivity of the copolymers. The flexibility and tensile strength of the EVM-*g*-PA6 copolymer were enhanced as compared to the corresponding EVM/PA6 blend. With the addition of 2.3 wt% of GO, the stress at 100% extension of the copolymer was enhanced by 190%, and Young's modulus was improved by 109%. The EVM-g-PA6 copolymer and the GO reinforced copolymeric nanocomposites would be developed to a new type of engineering thermoplastic elastomers.

Keywords Ester-amide exchange reaction; Elastomers; Nanocomposites

[1] *Corresponding author. Tel:* +86 21 54743257.
E-mail address: yong_zhang@sjtu.edu.cn (Y Zhang).

RSC Advances Accepted Manuscript

1. Introduction

Thermoplastic elastomers (TPEs) are polymer blends that contain chemically crosslinked polymer phase dispersed in continuous thermoplastic polymer matrix, or block copolymers with hard segment as the physically crosslink points dispersed in the soft segment polymer phase. TPEs can be produced via co-polymerization of monomers or dynamic vulcanization of polymer blends in the melt-compounding process. TPEs have found a broad range of applications in sports, transportation and engineering fields due to their diverse compositions, good melt-processability and elastic properties.[1]

Ethylene-vinyl acetate copolymer (EVA) has been used for modification of brittle polymers[2] and synthesis of new copolymers.[3-7] EVA/poly(butylene terephthalate) (PBT) blends was synthesized via a polymerization reaction of cyclic butylene terephthalate monomer (cBT) in the presence of EVA.[3] With the catalysis of titanium phenoxide, the ring-opening polymerization of cBT and the transesterification reaction between EVA and PBT occurred at the same time, leading to formation of up to 11.3 wt% of EVA-*g*-PBT copolymer. Polycaprolactone grafted EVA (EVA-*g*-PCl) and polylactide grafted EVA (EVA-*g*-PLA) prepared via *in situ* polymerization reactions produced 11 wt% and 8 wt% of the grafted copolymers, respectively.[4] The transesterification reaction between EVA and PLA produced up to 25 wt% of EVA-*g*-PLA copolymer in the presence of titanium oxides.[5] As the EVA-*g*-PLA yield increased, the elongation at break, Young modulus and biodegradability of the polymer blends were further enhanced. Barbosa and Moraes et al. synthesized poly(methyl methacrylate) grafted EVA (EVA-*g*-PMMA)[2] and polystyrene grafted EVA (EVA-*g*-PS)[6,7] by using partially hydrolyzed EVA and mercapto-modified EVA as the backbone, respectively. For the EVA-*g*-PMMA copolymer, the PMMA segments did not affect the crystallinity of EVA backbone. For the EVA-*g*-PS copolymer, the PS grafting efficiency of about 100% could be decreased as the molecular weight of the grafts increased, and broadening of the molecular weight distribution of the PS grafts reduced the compatibility to the EVA/PS polymer blends. The tensile strength of the compatibilized blends was increased with the increase of PS molecular weight in the copolymer. Hereinafter, the *in situ* formed graft copolymer offers a promising route to enhance the compatibility and mechanical properties of polymer blends.

TPEs with PA as the hard segments have been investigated either by *in situ* ring-opening polymerization of caprolactam (CL) in the presence of soft segments[8] or coupling reactions between PA and functionalized soft segments.[9] PA6 grafted EVA copolymers were obtained via aminolysis reaction of vinyl acetate groups with terminal amino groups of PA6 and coupling reaction between the terminal amino groups of PA6 and anhydride groups in the succinic anhydride grafted EVA.[10] An ester-amide exchange reaction between PA6

RSC Advances Accepted Manuscript

and ethylene-vinyl acetate rubber (EVM) was confirmed in our previous study and also illustrated in Scheme 1.[11-13]

Graphene oxide (GO) has been used to modify PA6 and PA6-based TPEs. For example, GO/PA6 nanocomposites were produced via *in situ* polymerization method.[14] The addition of GO reduced the average molecular weight of PA6 and acted as nucleation agent for α-form crystallinity while suppressing the formation of γ-form crystals of PA6. The degradation temperature of GO/PA6 was higher than that of neat PA6, and tensile strength was enhanced from 60.6 MPa for PA6 to 64.9 MPa with addition of 0.65 wt% of GO. PA6 based thermoplastic elastomers have been mainly produced by melt compounding methods. By tailoring the melt processing conditions, nanostructured PA6/fluoroelastomer blends were formed with weight average diameter of the dispersed elastomer phase in the range of 89-110 nm.[15] Graphite nanoplatelets reinforced PA6/elastomer blends were also reported.[16] Three types of elastomers: ethene-propene copolymer, ethene-methacrylate copolymer, and aminated polybutadiene, were directly melt-compounded with PA6 and graphite nanoplatelets. The graphite nanoplatelets were preferably located in the PA6 phase and caused a reduction of elastomer domain sizes. The combination of nanoplatelets, PA6 and elastomers resulted in enhanced strength, stiffness and toughness.

This work aims to syntheses EVM-*g*-PA6 copolymers directly from CL monomer and EVM polymer in order to maximize the grafting efficiency and simplify the reaction process. The reaction mechanism involving ring-opening polymerization of CL and ester-amide exchange reaction with EVM were proposed and studied. To enhance the graft efficiency, graphene oxide (GO), was used to facilitate the reactions. Dibutyltin oxide (DBTO) was selected as an esterification catalyst based on our previous study.[12] The effect of GO on the ester-amide exchange reaction between CL and EVM was studied, the crosslink-structure, electrical and mechanical properties of the resultant EVM-*g*-PA6/graphene nanocomposites were discussed.

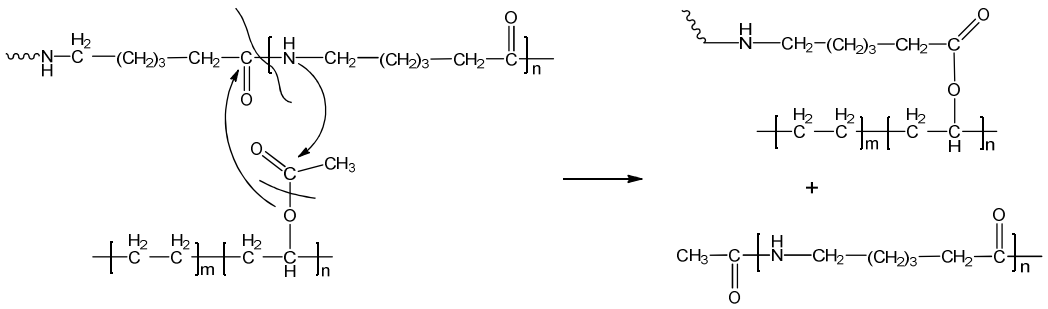

Scheme 1. Schematic diagram of ester-amide exchange reaction between PA6 and EVM.

RSC Advances Accepted Manuscript

2. Experimental

2.1. Materials

PA6 (1013B, $\overline{M_n} = 25{,}000\ g/mol$, relative viscosity of 2.3) was produced by UBE Chemical Co., Ltd., Japan. EVM (LEVAPREN 400) and EVM50 (LEVAPREN 500), $ML_{1+4}^{100℃} = 20$, has a vinyl acetate content of 40 wt% and 50 wt%, respectively. The Mooney viscosity ($ML_{1+4}^{100℃}$) is measured by Mooney Viscometer, reflecting polymerization degree and molecular weight of synthetic rubbers, where M represents Mooney and L represents the large rotor. The viscosity is measured with preheating time of 1 minute and testing time of 4 minutes under 100 °C. Both EVM elastomers were kindly supplied by Lanxess Deutschland GmbH, Germany. Dibutyltin oxide (DBTO, 98%) and deuterated solvents ($CDCl_3$ and CF_3COOD) were purchased from Adamas-beta Reagent Co., Ltd., Switzerland. Caprolactam (CL, C.P.), aminocaproic acid (ACA, 98.5%), formic acid (88%) and N-methyl acetamide (NMA, 99.9%) were purchased from Sinopharm Group Chemical Reagent Co., Ltd., China. Flake graphite (99.8%) with average particle size of 45 μm was purchased from Alfa Aesar company. $CHCl_3$, xylene, methanol, $KMnO_4$, concentrated H_2SO_4, concentrated HCl and H_2O_2 aqueous solution (30 wt%) were all analytical grade and purchased from Sinopharm Chemical Reagent Co. Ltd., China.

2.2. Sample preparation

2.2.1. Ester-amide reaction polymerization

Briefly, a mixture of 24.0 g EVM (0.1116 mol VA), 36.0 g CL (0.3181 mol), 1.94 g ACA (0.01479 mol) and 0.6 g (1 wt% of the blends) DBTO were added into a 100 mL three-neck flask equipped with a mechanical stirrer, reflux condenser and continuous nitrogen flow. After the melting of CL at 80 °C, the mixture was heated up to 180 °C for 4 h and 230 °C for 4 h under refluxing. A series of reaction mixtures at varied reaction conditions were prepared in order to investigate the effects of reaction time and amide/ester ratio on the grafting polymerization efficiency.

2.2.2. Preparation of PA6/EVM blend

PA6 and EVM were firstly vacuum-dried for 12 h at 100 °C and 60 °C, respectively, then mixed and compounded by using a Haake rheometer with a rotor speed of 60 rpm. The resultant blends were vacuum-dried at 80 °C for 12 h and then compressed into specimens at 240 °C for tensile testing.

2.2.3 Preparation of EVM-g-PA6 copolymer/Graphene (TPE-G) Composites

RSC Advances Accepted Manuscript

GO was prepared using a modified Hummers method from flake graphite.[17] A typical procedure to prepare TPE/graphene composites was depicted as follows: GO (60 mg, 0.1 wt% of the blend) and CL (48 g, 0.42 mol) were added into a 100 mL three-neck round-bottom flask and the mixture was stirred at 80 °C for 2 h, followed with ultrasonication at 80 °C for 2 h. EVM (12 g, 0.056 mol), ACA (2.59 g, 0.0197 mol) and DBTO (0.6 g, 0.002 mol) were then added to the above solution. The mixture was kept stirring at 80 °C for 30 min under nitrogen flow and then heated at 180 °C for 1 h and 230 °C for 5 h (The reaction condition was optimized from our previous study[12]). After cooling to room temperature, the reaction mixture was chopped into small pieces and ready for further testing.

2.2.4. Solvent-extraction of the copolymer

The extraction procedure is summarized in Scheme 2. Briefly, 15 g samples was dissolved in 250 mL formic acid at room temperature. The insoluble part was filtrated and washed with formic acid for several times. The solution obtained was precipitated in methanol to obtain Fraction I (PA6 homopolymer), which was further washed with methanol and vacuum dried at 60 °C for 24 h. The insoluble part was vacuum-dried at 60 °C for 48 h, then dissolved in xylene for 24 h. The suspension was then filtrated, and the residue of the insoluble part was vacuum-dried at 60 °C for 48 h to obtain Fraction III (EVM-*g*-PA6 copolymer). The clear solution was evaporated to get Fraction II (unreacted EVM). The copolymer/GO nanocomposites were extracted following the same procedure, the resultant Fraction III' was named as TPE-G-*x*, where *x* is the graphene weight percentage.

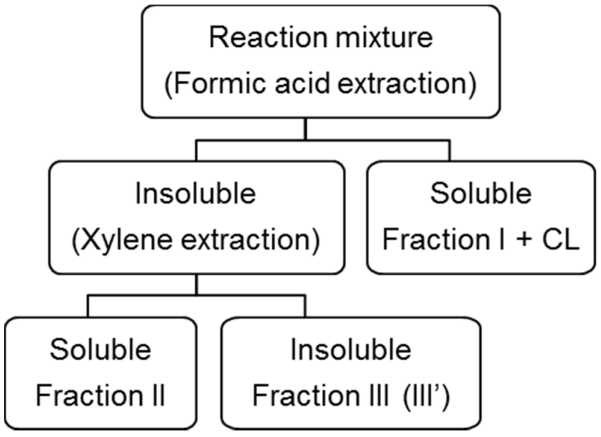

Scheme 2. Solvent extraction of the copolymer from the EVM/CL mixture after polymerization.

2.3. Characterization

Infrared spectra of samples were obtained by using a Spectrum 100 Fourier transform infrared spectrometer (FTIR, Perkin Elmer, Inc., USA). The wave number is ranged from 450 to 4000 cm^{-1}. Thermal analysis was

RSC Advances Accepted Manuscript

carried out on a differential scanning calorimeter (DSC, Q2000, TA Instruments, USA). All the samples were firstly heated from 40 to 240 °C to eliminate previous thermal history and crystallization, then cooled down to -70 °C, and finally heated up from -70 to 240 °C. Thermograms were recorded during both heating and cooling cycles at 10 °C/min in nitrogen. The glass transition temperature and melting behavior of the components were determined from the second heating run. Thermogravimetric analysis (TGA) was carried out by using a thermogravimetric analyzer (Q5000, TA Instruments, USA). All the samples were vacuum-dried overnight. The samples were heated from room temperature to 110 °C under nitrogen atmosphere and hold isothermal for 5 min, then further heated up to 700 °C at 20 °C/min. Liquid ^{1}H NMR spectra were recorded by a MERCURY plus 400 (Varian, Inc., USA) using $CDCl_3$/CF_3COOD (1/1 v/v) as a solvent. Chemical shifts were given in ppm in reference to internal tetramethylsilane (TMS).

The grafting degree of PA6 to EVM was determined by elemental analysis of the EVM-*g*-PA6 copolymer in an Elemental Analysis-Stable Isotope Ratio Mass Spectrometer (Vario EL III/Isoprime, Elementar Co., Ltd., Germany). The PA6 content in the EVM-*g*-PA6 copolymer can be estimated from the equation of PA6 content = 113*x*/14, while *x* is the nitrogen content in the copolymer. X-ray photoelectron spectroscopy (XPS) was carried out on an AXIS ULTRA DLD instrument (Kratox, Japan) with Al Kα radiation ($h\nu$ = 1486.6 eV). X-ray diffraction (XRD) patterns were recorded on a D/max-2200/PC X-ray diffractometer (Rigaku Co., Japan) at 40 kV, 40mA, scanning rate of 4 °/min, scanning range from 5° to 60°. The samples of 18 × 18 × 1 mm^3 sheets were compression-molded at 230^{o}C.

The dispersion of graphene in the EVM-*g*-PA6/graphene composites was observed from the cryogenically fractured surface of the specimens using scanning electron microscopy (SEM, Nova NanoSEM, FEI Co., Ltd., USA). Atomic force microscopy (AFM) was carried out in tapping mode on a Nano Scope III A (Digital Instrument, USA). The cantilevers had a spring constant of 40 Nm^{-1} and a resonance frequency of 300 kHz. The GO/H_2O and TPE-G/($CHCl_3$/CF_3COOH, 1/1 v/v) solutions were spin-coated onto freshly exfoliated mica substrates at 2000 rpm and dried in fume hood. The copolymer samples were cryo-sectioned into 10 nm-thick sections and stained with vapor of 1 wt% ruthenium tetroxide (RuO_4) solution for 30 min at room temperature, then observed using a JEM 2100 transmission electron microscopy (TEM, JEOL Ltd., Japan).

The volume resistivity of EVM-*g*-PA6/graphene composites was measured according to ASTM D 257 on an EST121 high resistance meter. The specific volume resistivity was calculated according to $\rho_v = R_v \cdot \frac{\pi(D+g)^2}{4t}$, where ρ_v is the specific volume resistivity, R_v is the volume resistivity and t is the thickness

RSC Advances Accepted Manuscript

of specimen. D=5.0 cm, the diameter of inner circular electrode, g=0.2 cm, the gap width between inner and outer circular electrodes. The volume conductivity of samples was further calculated from the reciprocal of volume resistivity. Dielectric properties of EVM-*g*-PA6/graphene composites were measured by using a Concept 40 broadband dielectric spectrometer (Novocontrol, Germany) with Alpha - Beta Analyzer at 23 ℃. Before testing, all the samples were kept at the room temperature of 23 ℃ for at least 8 h. The applied alternating current (AC) voltage was 1 V and the frequency range was from 10^{-1}~10^{7} Hz. The sample was about 0.2 mm in thickness and the round movable plate electrode was 10 mm in diameter. The dielectric permittivity (ε), dielectric loss factor (tanδ) and AC conductivity (σ) of the composites were recorded.

Tensile testing was measured by using a universal test machine (Instron 4465, USA) at a crosshead speed of 500 mm/min for the EVM-*g*-PA6 copolymer and PA6/EVM blend following ASTM D412. The testing environment temperature is 23±1 ^{o}C, relatively humidity is 55%. The dumbbell specimens with dimensions of 75 mm in length, 0.2 mm in thickness and 4 mm in width, were prepared by compression molding at 230 ℃. The samples were placed at 23±1 ^{o}C and relatively humidity of 55% for over 4h, then 5 specimens were tested for each sample.

3. Results and discussion

3.1. Synthesis and characterisation of EVM-g-PA6 copolymers

Graft copolymers have been synthesized by various methods, such as transesterification,[4,5] free radical polymerization,[18,19] click chemistry,[20] melt-coupling reactions, reactive compounding,[7] and *in situ* polymerization of monomer in the presence of polymers.[3,4,10] Recently, a combination of free radical polymerization and polycondensation approach[21,22] has been developed to enrich the chemical structures of graft copolymers. In this study, a new graft copolymer EVM-*g*-PA6 was directly prepared through a simultaneous polymerization reaction of CL to PA6 and exchange reaction with EVM at mild conditions, which highly simplifies the synthesis procedures of EVM-g-PA6 copolymers, as the EVM and PA6 are generally made via free radical polymerization and ring-opening polymerization reaction, respectively. The ester-amide exchange reaction mechanism is proposed and described in Scheme 3.

RSC Advances Accepted Manuscript

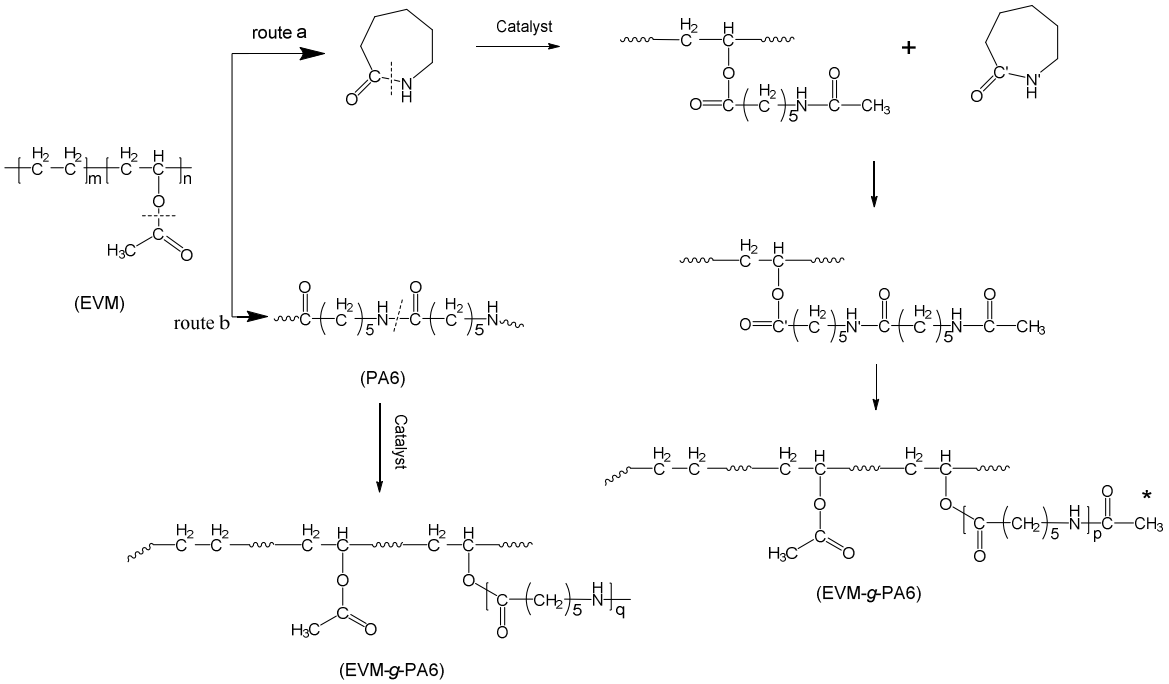

Scheme 3. The schematic diagram of catalyzed grafting polymerization of CL onto EVM.

To determine the chemical structure of the reaction product, the resultant insoluble residue (EVM-g-PA6 copolymer, Fraction III in Scheme 2) separated via a solvent-extraction method was characterized by using ^{1}H NMR (Fig. 1a). It is found that both the insoluble residue and the reaction mixture show signals at 2.65 and 3.45 ppm, corresponding to the chemical shifts of methyl protons adjacent to carbonyl group and amino group of PA6, respectively. Two additional signals at 2.18 and 4.98 ppm are observed in the ^{1}H NMR spectrum of Fraction III as compared to that of PA6, which are assigned to methyl and methine protons of EVM. The characteristic signals of CL monomer can be detected from the spectrum of the reaction mixture, indicating only partial CL monomers participated in the polymerization reaction. The intensity of characteristic signals (a and b) of PA6 were reduced after extraction, indicating part of PA6 was extracted by formic acid. That is, CL monomer took part in two reactions: graft-copolymerisation forming EVM-g-PA6 copolymer, and homopolymerisation forming PA6 which can be extracted by formic acid. The characteristic signals of PA6 in the extracted residue mean those grafted PA6 to EVM (EVM-g-PA6). The peak at 2.40 ppm assigned to the methyl protons adjacent to amide carbonyl group is spotted in the ^{1}H NMR spectrum of EVM-*g*-PA6 copolymer (Fraction III), which reflects its molecular structure as proposed in Scheme 3. The FTIR characterisation results (Fig. 1b) of the copolymer exhibit absorption peaks at 1739 cm^{-1} (assigned to C=O), 1638 cm^{-1} (NHC=O), 1545 and 3300 cm^{-1} (N-H), and 1260-1280 cm^{-1} (C-N), indicating the coexistence of EVM and PA6 structure in the copolymer. Therefore, CL should self-polymerized into PA6 as well as take part in the

RSC Advances Accepted Manuscript

ester-amide exchange reaction with EVM to produce EVM-*g*-PA6 copolymer. In addition, the exchange reaction between EVM and PA6 homopolymer also contributes to the formation of EVM-*g*-PA6 copolymer.

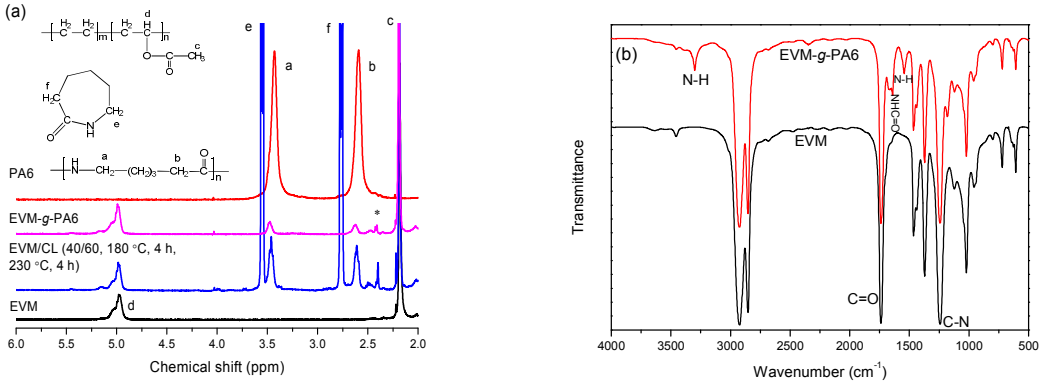

Fig. 1. (a) ^{1}H NMR spectra of PA6, EVM, reaction mixtures and the extracted copolymer; (b) FTIR spectra of the extracted copolymer from EVM/CL (40/60, 180 °C for 4 h and 230 °C for 4 h).

The extracted fractions from the reaction mixture of EVM/CL (40/60, 180 °C for 4 h and 230 °C for 4 h) are listed in Table 1. The polymerization conversion of CL is 15%, which is calculated from the ^{1}H NMR spectrum of reaction mixture through the ratio of characteristic signal intensity of PA6 (homopolymerized PA6 and PA6 in EVM-*g*-PA6) to that of unreacted CL. The copolymer yield is 26.4 wt%, which is obtained from the weight fraction of the copolymer (Fraction III) in the reaction mixture. The melting temperatures as determined from DSC thermograms (Fig. 2) are 205 °C for the copolymer and 174 °C for the homopolymerized PA6, respectively. Both the melting temperature and enthalpy of the PA6 branches in the copolymer are increased with the increase of polymerization time and the amide/ester ratio ([CL]/[VA]) as shown in Fig. S1. The higher melting temperature of the PA6 branches is indicative of the longer chains of grafted PA6 branches.

Table 1 The extraction fractions of EVM/CL reaction mixture (40/60, 180 °C for 4 h and 230 °C for 4 h).

Fraction	PA6	EVM	CL	EVM-*g*-PA6	[a]CL conversion	[b]CL conversion
wt%	7.9	15.7	49.0	26.4	14.9	16.8

[a] calculated from selection extraction results; [b] calculated from ^{1}H NMR results.

RSC Advances Accepted Manuscript

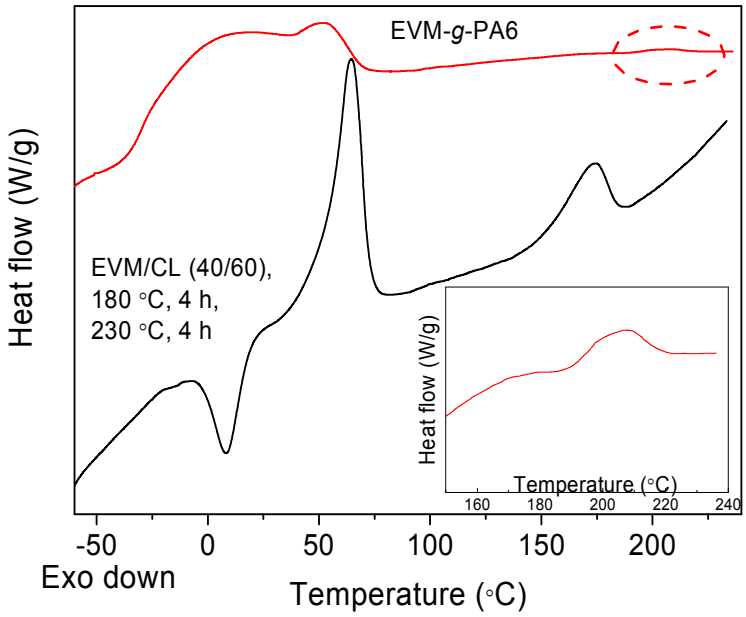

Fig.2. DSC thermograms of EVM/CL (40/60, 180 °C for 4 h and 230 °C for 4 h) reaction mixture and the extracted copolymer.

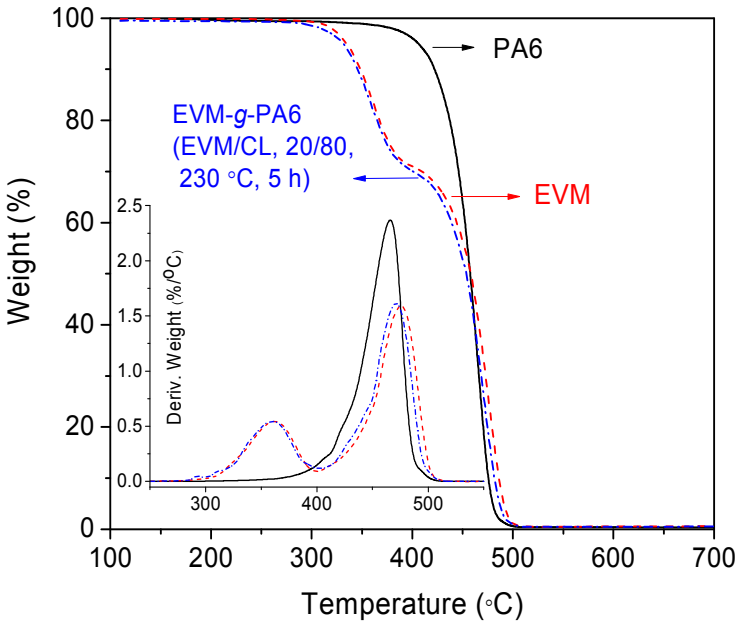

Fig. 3. TGA and DTG thermal curves of PA6, EVM and the EVM-*g*-PA6 copolymer.

The number average molecular weight ($\overline{M_n}$) of grafted PA6 branches in the copolymer is estimated by the

RSC Advances Accepted Manuscript

ratio of the characteristic proton signal intensity of PA6 branchs to the proton signal intensity of methane group bonded to the PA6 branches, according to $\overline{M_n} = \frac{I_{3.45} M_A}{2\left(I_{4.97} - I_{2.18}/3\right)}$, where M_A is the molar mass of structure unit of PA6, $I_{3.45}$, $I_{4.97}$ and $I_{2.18}$ are the intensity ratio between the characteristic proton signal peaks the copolymer at 3.45 ppm, 4.97 ppm and 2.18 ppm, respectively. The $\overline{M_n}$ of grafted PA6 branches in the copolymer is estimated to be 1162 g/mol as calculated by the ratio of the characteristic proton signal intensity of PA6 branch to the proton signal intensity of methane group bonded with PA6 branches as illustrated in the ^{1}H NMR spectra (Fig.1a). It is estimated to be 4000 g/mol by using a DSC method.[9] The difference in the estimated molecular weight of the PA6 branches implies a polydispersity of the molecular weight. The EVM-*g*-PA6 copolymer exhibits two degradation steps as characterized by TGA (Fig. 3). The first degradation at 330~400 °C is similar to that of EVM (elimination of the acetate groups, 28.8 wt%) but with slightly higher weight loss of 29.9 wt%. In the temperature range of 440~500 °C, the initial decomposition temperature (449.7 ^{o}C) and peak temperature of decomposition rate (471.3 ^{o}C) of the copolymer are between those of PA6 (436.8 ^{o}C, 465.9 ^{o}C) and EVM (450.3 ^{o}C, 475.7 ^{o}C), which suggests that the degradation of the long PA6 branches and the EVM backbone.

The graft PA6 branches are also quantified with elemental analysis. As shown in Table S1, For EVM/CL weight ratio of 20/80, the grafted PA6 content is increased from 4.0 to 5.6 wt% with the reaction time increasing from 5 to 8 h. As the EVM/CL weight ratio is increased from 20/80 to 40/60, the PA6 content is increased from 4.0 to 5.7 wt%, but the melting temperature of the graft PA6 branches is decreased from 214~218 to 206~215 °C. Therefore, higher amide/ester ratio and longer reaction time favor the grafting polymerization of PA6.

3.2. Effects of GO on the copolymerization of EVM-g-PA6

In order to facilitate the exchange reaction between EVM and CL monomer and improve the yield of EVM-*g*-PA6 copolymer, GO was introduced into the reaction mixture with loadings of 0.1, 0.5, or 1.0 wt%. The prepared GO nanosheets are about 3 μm in length and 0.9 nm in thickness (Fig. S2a), the C/O atomic ratio is about 2.3 as estimated from the three oxygen-containing groups (C-OH, C-O-C and C=O (COOH)) in GO (XPS spectrum, Fig. S2b).[23] About 55 wt% of oxygen-containing groups was evaluated according to the elimination amount in the heating process of TGA (Fig. S2c).

RSC Advances Accepted Manuscript

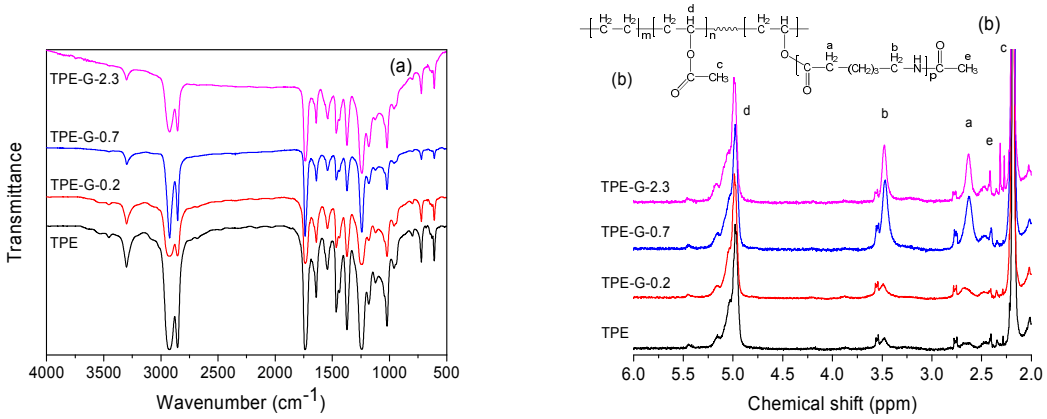

Fig. 4. FTIR (a) and ^{1}H NMR (b) spectra of the extracted copolymer/graphene composites.

The ester-amide exchange reaction between CL and EVM to produce EVM-*g*-PA6 copolymer in the presence of GO is proposed in Scheme 4. The hydroxyl and carboxyl groups on the GO surface may promote the polymerization of CL[24] to form PA6 grafted graphene, which will further take part in the exchange reaction with EVM to form EVM-*g*-PA6 grafted graphene (TPE-G) composites.

To justify this reaction mechanism, the reaction products were selectively extracted following the procedure as shown in Scheme 2. The final extraction residues (Fraction III') could form stable dispersions in formic acid and $CHCl_3/CF_3COOH$ (1/1 v/v), respectively (Figure S3), reflecting the existence of PA6 and EVM-g-PA6 copolymer on the GO surface and thus improved the dispersability of GO in the organic solvents.

The graphene concentration in the copolymers was determined to be 0.2, 0.7 and 2.3 wt% by TGA, respectively (Fig. S4). The extracted copolymers were also characterized by FTIR (Fig.4a) and ^{1}H NMR (Fig. 4b). The characteristic absorption peaks at 1739 cm^{-1} (assigned to OC=O), 1638 cm^{-1} (NHC=O), 1545 and 3300 cm^{-1} (N-H), and 1260-1280 cm^{-1} (C-N) observed from the copolymer indicate the coexistence of EVM and PA6 structures. In the ^{1}H NMR spectra, the copolymers show the characteristic signals of both PA6 and EVM. The graft PA6 content is determined to be 13.1 wt% for TPE-G-0.7 via elemental analysis, while it is 6.0 wt% for the copolymer (Table S2). This suggests that GO could facilitate the CL polymerization and meanwhile take part in the exchange reaction between PA6 and EVM, so that some PA6 chains were grafted onto the graphene sheets where some copolymers were also attached to the graphene surface (Scheme 4). This indicates that more PA6 was indirectly connected to the copolymers through the graphene sheets, thus resulting an increased the grafting amount of PA6 in the copolymeric composites.

RSC Advances Accepted Manuscript

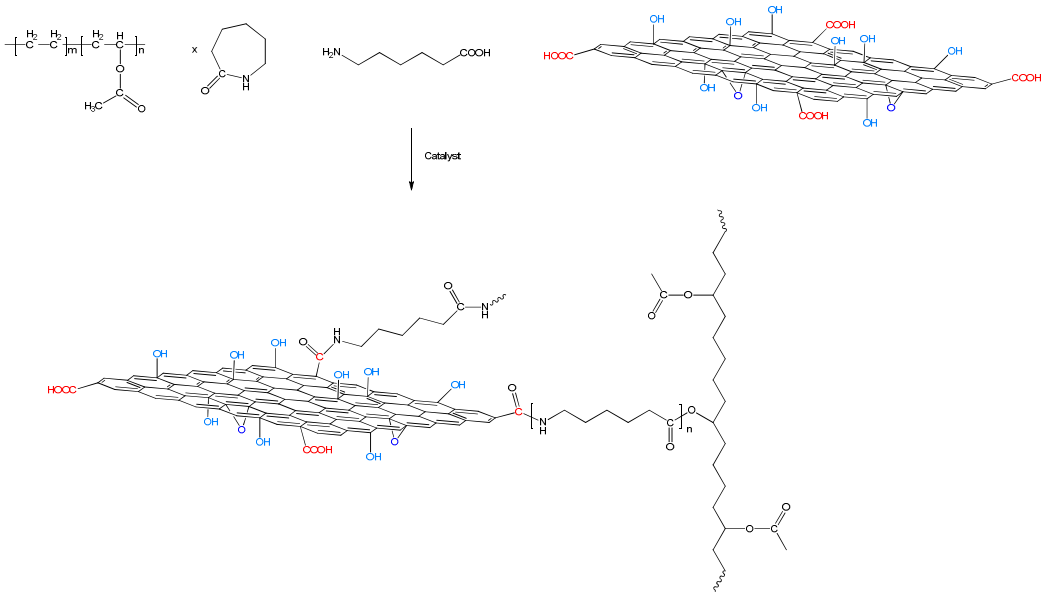

Scheme 4. Schematic diagram of catalyzed grafting polymerization of CL onto EVM via an ester-amide exchange reaction in the presence of GO.

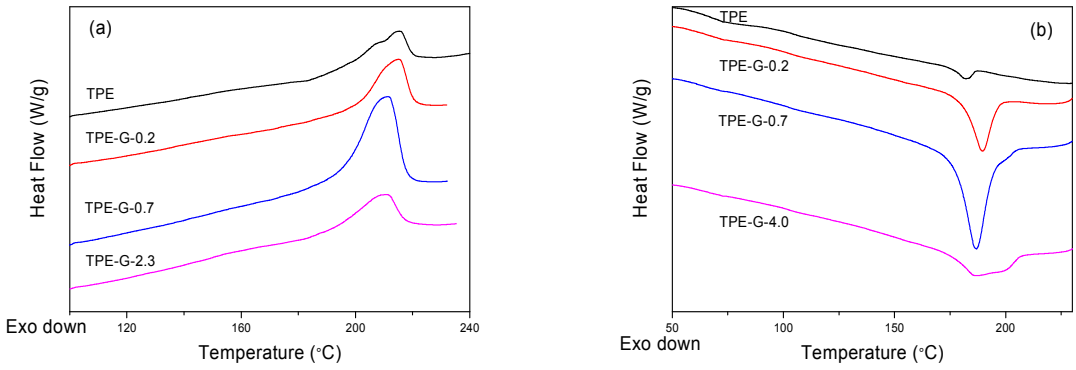

Fig. 5. DSC heating scanning (a) and cooling scanning (b) curves of the extracted copolymer/graphene composites.

The molecular weight of EVM-*g*-PA6 copolymer can not be directly measured due to its poor solubility. Here we use the melting temperature of PA6 branches to reflect the PA6 branch length in the copolymer. Generally a higher molecular weight indicates a higher melting point[9] for homopolymers. In the case of EVM-g-PA6 graft copolymers, the amorphous EVM backbone may affect the crystallization rate of PA6 branch chains, but should not affect the melting temperatures. The variety of the molecular weight should be mainly caused by the length of PA6 branches. Therefore, the melting points were measured to indirectly reflect the change of the molecular weight of PA6 branches. As shown in Fig. 5 and Table S3, the melting temperature of EVM-*g*-PA6 copolymer is about 215.3 °C. It is assigned to the grafted PA6 [25] and can be used

RSC Advances Accepted Manuscript

to reflect a number average molecular weight of 5000~6000 g/mol.[9] With addition of GO up to 2.3 wt%, the melting temperature was decreased to 210.8 °C, corresponding to a number average molecular weight of about 4000 g/mol. In addition, the crystallization temperature and crystallization enthalpy were increased after the introduction of GO. This should be caused by the heterogeneous nucleation effect of graphene.[26-28] As the GO content was increased from 0.2 to 2.3 wt%, the crystallization temperature and crystallization enthalpy of the copolymers were decreased due to the increasing restriction of the graphene sheets on the crystal growth but the crystal structure of PA6 was not changed as shown from XRD patterns in Fig. S5.

3.3. Morphology of EVM-g-PA6 copolymers and nanocomposites

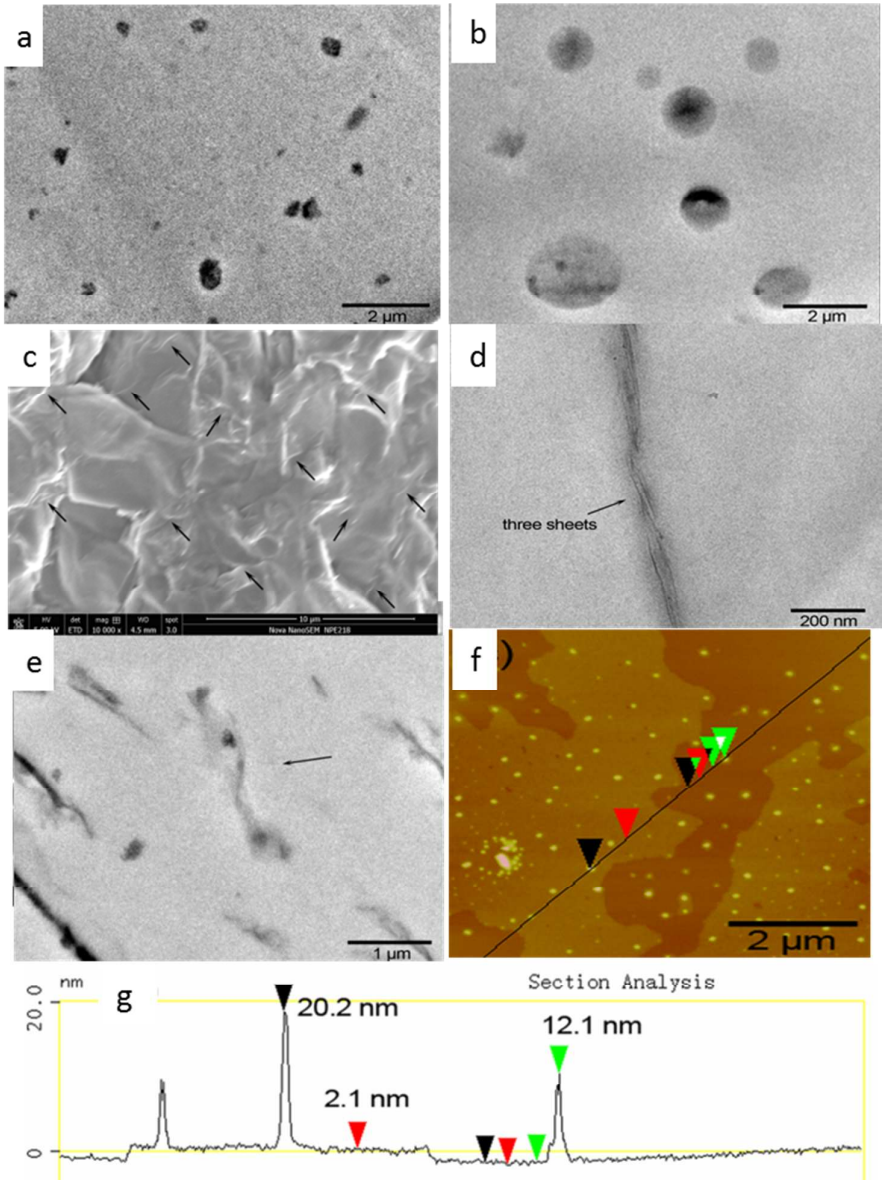

RSC Advances Accepted Manuscript

Fig. 6. (a) TEM image of EVM-g-PA6 extracted from EVM/CL(40/60, 180 °C, 4 h, 230 °C, 4 h); (b) EVM/PA6 (95/5)blend; (c) SEM image of cryogenically fractured surface of TPE/graphene composites with graphene content of 0.7 wt% (The arrows mark the graphene sheets); (d, e) TEM images of TPE/graphene composite with 0.7 wt%; (f) tapping mode AFM image and (g) the height profile of TPE/graphene composite with 0.7 wt% graphene.

Microphase separation is often observed in block copolymers and graft copolymers. The disorder-to-order transition is driven by the difference in solubility parameters between polymer components, and leads to ordered arrays of regular domains with diameter of about several tens of nanometers. For the EVM-*g*-PA6 copolymer, the difference in molecular polarity between EVM and PA6 results in microphase separation as shown in Fig. 6a. The PA6 phase (dark particles stained by RuO_4) with an average particle size of about 200 nm in diameter was dispersed in the EVM matrix (bright area) in the EVM-*g*-PA6 copolymer, which is much smaller than that observed in the EVM/PA6 (95/5) blend (about 1500 nm in diameter, Fig. 6b).

The graphene sheets exhibit good interfacial adhesion with polymers (Fig. 6c) and are distributed as few layers throughout the polymer matrix (Fig. 6d). This may be caused by the faster thermal reduction of GO at the reaction temperature than that of reactions between GO and polymers, so that some graphene sheets may congregate in the molten CL before participating in the reactions.

As shown in Figure 6e for TPE-G-0.7, some black dots with diameter of about 200 nm were observed on GO surface, which is similar to that of grafted PA6 domans in the copolymer (Fig.6a). The thickness of the graphene sheets was increased from 0.9 to about 2 nm (Fig. 6f and 6g) suggesting the grafting polymers on the graphene surface.[29] As depicted in Scheme 4, the hydroxyl and carboxyl groups in the GO take part in the exchange reaction with EVM and polymerization reaction of CL. As a result, the PA6 homopolymer and copolymer grafts would be connected through graphene sheets. This further complements the ^{1}H NMR and FTIR results (Fig. 1 and Fig. 2). The separated PA6 and copolymer on the graphene sheets have a conical shape with about 12 nm and 20 nm in height, respectively, which are higher than those of polyphenylene oxide (7 nm) in polyphenylene oxide-GO hybrids prepared through π-π stacking.[29]

3.4.Mechanical and electrical properties

The tensile properties of the EVM-*g*-PA6 copolymer were compared with the corresponding EVM/PA6 blend. As shown in Table 2 and Fig. 7, the tensile strength and stresses at 100% extension of the copolymer are higher than those of EVM and EVM/PA6 blend. The fracture tensile strength of the copolymer is 12.9

RSC Advances Accepted Manuscript

MPa with a corresponding elongation at break of 693%. With the increase of PA6 content, the stresses at 100% and 200% extension and set at break increase (Fig. S7).

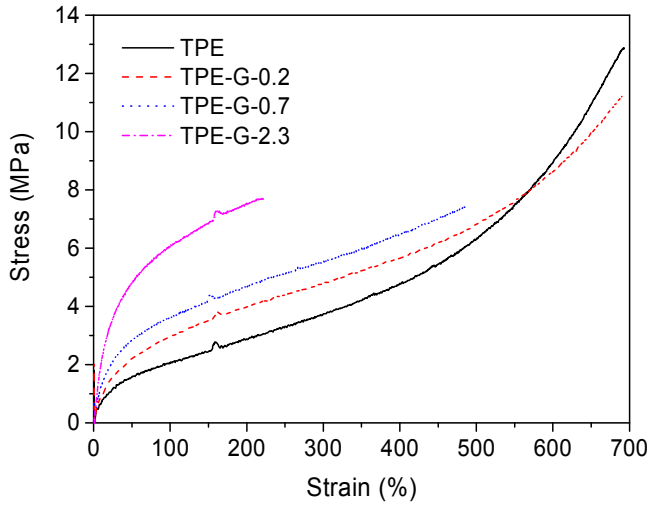

Fig.7. Tensile stress-strain curves of TPE/graphene composites.

With the addition of 2.3 wt% of graphene, the stress at 100% extension of EVM-g-PA6 copolymer was increased from 2.1 to 6.1 MPa (Fig. 7). The reinforcement effect of graphene to the copolymer is attributed to the high stiffness of graphene as well as the increased PA6 content due to the catalytic effect of graphene. The graphene sheets link PA6 branches and EVM-g-PA6 copolymers together, thus forming a crosslinking network in the copolymer composites. Therefore, the stress at 100% extension and the modulus of the composites were greatly increased, although the elongation at break was decreased due to the increased stiffness of the composite structure.

Table 2 Physical properties of TPE/graphene composites.

TPE/graphene composites	Young's modulus (MPa)	Tensile strength (MPa)	Stress at 100% extension (MPa)	Stress at 200% extension (MPa)	Elongation at break (%)	Set at break (%)	σ_v (S/cm)
EVM	-	8.2±0.3	1.2±0.1	1.9±0.3	820±15	>100	$\sim 10^{-15}$
EVM/PA6 blend (95/5)	-	5.0±0.2	2.0±0.3	3.0±0.2	677±22	>100	$\sim 10^{-15}$
TPE[a]	15.2±0.5	12.9±0.6	2.1±0.2	2.9±0.2	693±23	90±21	1.84×10^{-15}
TPE-G-0.2	22.6±0.9	11.2±0.5	3.0±0.4	4.0±0.3	689±34	100±18	3.23×10^{-15}
TPE-G-0.7	24.8±1.3	9.7±0.6	3.6±0.3	4.7±0.4	487±36	65±12	5.76×10^{-13}

RSC Advances Accepted Manuscript

TPE-G-2.3	31.7±2.5	7.7±2.1	6.1±1.2	7.5±0.5	220±30	15±4	5.49×10^{-8}

[a] TPE is EVM-*g*-PA6 copolymer (EVM/CL, 40/60, 180 °C, 4 h, 230 °C, 4 h)

For EVM-g-PA6/graphene composites, the percolation threshold is reached in between 0.7 ~ 2.3 wt% of graphene, where the real permittivity is generally independent of frequency and exhibits great fluctuation at low frequencies (10^0 - 10^3 Hz) due to the good conducting performance (Table 2 and Fig. 8a). The DC and AC conductivity was increased about 7 orders of magnitude when the graphene content was increased to 2.3 wt%. The permittivity and dielectric loss of the copolymer were also increased greatly with the addition of graphene (Fig. 8b and Fig. S8).

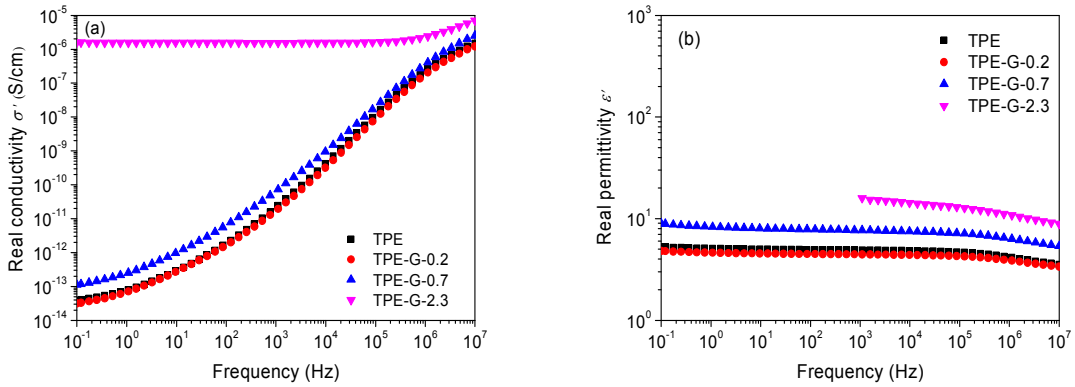

Fig. 8. Dielectric parameters of EVM-*g*-PA6 copolymer/graphene composites as a function of frequency at room temperature: (a) real conductivity and (b) real permittivity.

4. Conclusion

EVM-*g*-PA6 copolymer was synthesized via an ester-amide exchange reaction between CL monomer and acetate groups of EVM. The polymerization conversion of CL is about 15% and the copolymer yield is about 26.4 wt% in the CL/EVM (60/40) mixture under the condition of 180 °C for 4 h and 230 °C for 4 h. The obtained copolymer contains 4~6 wt% of PA6 with a wide molecular weight distribution and shows melting temperatures of 205~220 °C. Higher grafting ratio of the PA6 in the EVM-*g*-PA6 copolymer can be obtained by increasing the reaction time or decreasing the amide/ester ratio. The addition of GO facilitates the graft polymerization of both PA6 and copolymers, the GO sheets were simultaneously thermally reduced to graphene during the polymerization process. With incorporation of 0.7 wt% graphene, the PA6 content in the EVM-*g*-PA6 copolymer was increased from 6.0 up to 13.1 wt%. The PA6 homopolymer and EVM-*g*-PA6 copolymer were covalently linked together through graphene sheets. Such covalent-crosslinked structure is beneficial to a higher mechanical strength and a lower percolation threshold in electrical conductivity of the

RSC Advances Accepted Manuscript

composites. The stress at 100% extension of EVM-*g*-PA6 was enhanced from 2.1 up to 6.1 MPa, and the volume conductivity and permittivity were also increased significantly. As compared to commercial PA6-based TPEs which are generally block-copolymers, the EVM-g-PA6 TPEs are grafted copolymers. This will favor the formation of phase-separation morphology so that benefit mechanical and thermal properties. The novel thermoplastic elastomeric nanocomposites with balanced mechanical, oil-resistant and thermal-resistant properties have shown great potential in engineering applications.

Acknowledgement

This work was supported by the National Natural Science Foundation of China (grant No. 51073092).

References

[1] K. Naskar, J.W.M. Noordermeer, Prog. Rubber. Plast. Re. 21 (2005) 1-26.

[2] M.A.R. Moraes, A.C.F. Moreira, R.V. Barbosa, B.G. Soares, Macromolecules 29 (1996) 416-422.

[3] W. Bahloul, V. Bounor-Legaré, F. Fenouillot, P. Cassagnau, Polymer 50 (2009) 2527-2534.

[4] I. Moura, R. Nogueira, V. Bounor-Legare, A.V. Machado, React. Funct. Polym. 71 (2011) 694-703.

[5] I. Moura, R. Nogueira, V. Bounor-Legare, A.V. Machado, Mater. Chem. Phys. 134 (2012) 103-110.

[6]R.V. Barbosa, B.G. Soares, A.S. Gomes, J. Appl. Polym. Sci. 47 (1993) 1411-1418.

[7] R.V. Barbosa, B.G. Soares, A.S. Gomes, Macromol. Chem. Phys. 195 (1994) 3149-3157.

[8] L.L. Hou, H.Z. Liu, G.S. Yang, Polym. Int. 55 (2006) 643-649.

[9] C. Yi, Z. Peng, H. Wang, M. Li, C. Wang, Polym. Int. 60 (2011) 1728-1736.

[10] B. Immirzi, M. Malinconico, E. Martuscelli, Polymer 32 (1991) 364-373.

[11] W. Wu, C. Wan, S. Wang, Y. Zhang, RSC Advances 3 (2013) 26166-26176.

[12] W. Wu, C. Wan, H. Zhang, Y. Zhang, J. Appl. Polym. Sci. 131 (2014) Doi: 10.1002/app.40272.

[13] W. Wu, C. Wan, S. Wang, Y. Zhang, Polym. Bull. 71 (2014) 1505-1521.

[14] D. Dixon, P. Lemonine, J. Hamilton, G. Lubarsky, E Archer, J. Thermop. Comp. Mater. 2013, doi: 10.1177/0892705713484749.

[15] S. S. Banerjee, A. K. Bhowmick, Polymer, 54 (2013) 6561-6571.

[16] T.T. Duy, L. Kapralkova, J. Hromadkova, I. Kelnar. Euro. Polym. J. 50 (2014) 39-45.

[17] W.S. Hummers, R.E.Offeman, J. Am. Chem. Soc. 80 (1958) 1339-1339.

[18] L. Jiang, W. Huang, X. Xue, H. Yang, B. Jiang, D. Zhang, J. Fang, J. Chen, Y. Yang, G. Zhai, L. Kong, S. Wang, Macromolecules 45 (2012) 4092-4100.

RSC Advances Accepted Manuscript

[19] C. Nakason, A. Kaesaman, A. Rungvichaniwat, K. Eardrod, S. Kiatkamjonwong, J. Appl. Polym. Sci. 89 (2003) 1453-1463.

[20] P. Zhao, Y. Yan, X. Feng, L. Liu, C. Wang, Y. Chen, Polymer 53 (2012) 1992-2000.

[21] J. Liu, F. Zhan, Q. Fu, X. Zhu, W. Shi, J. Polym. Sci. Part A: Polym. Chem. 46 (2008) 7543-7555.

[22] Y.-C. Liu, W. Xu, Y.-Q. Xiong, F. Zhang, W.-J. Xu, Mater. Lett. 62 (2008) 1849-1852.

[23] Y. Xing, X. Bai, Y. Zhang, Polym. Compos (2013) Doi: 10.1002/pc.22831.

[24] Z. Xu, C. Gao, Macromolecules 43 (2010) 6716-6723.

[25] W. Hou, B. Tang, L. Lu, J. Sun, J. Wang, C. Qin, L. Dai, RSC Adv., 4 (2014), 4848-4855.

[26] L. Hua, W. Kai, J. Yang, Y. Inoue, Polym. Degrad. Stab. 95 (2010) 2619-2627.

[27] Z. Yang, H. Lu, J. Appl. Polym. Sci. 128 (2013) 802-810.

[28] X. Zhang, X. Fan, H. Li, C.Yan, J. Mater. Chem. 22 (2012) 24081-24091.

[29] Y. Cao, J. Zhang, J. Feng, P. Wu, ACS Nano. 5 (2011) 5920-5927.

RSC Advances Accepted Manuscript